J|A|C|S
ARTICLES

Published on Web 03/19/2010

Controlled Storage of Ferrocene Derivatives as Redox-Active Molecules in Dendrimers

Yousuke Ochi,[†] Mana Suzuki,[†] Takane Imaoka,[†,§] Masaki Murata,[‡] Hiroshi Nishihara,[‡] Yasuaki Einaga,[†] and Kimihisa Yamamoto*[,†,§]

Department of Chemistry, Faculty of Science and Technology, Keio University, Yokohama 223-8522, Japan and Department of Chemistry, School of Science, The University of Tokyo, 7-3-1 Hongo, Bunkyo-ku, Tokyo 113-0033, Japan

Received September 14, 2009; E-mail: yamamoto@res.titech.ac.jp

Abstract: Dendritic polyphenylazomethines (**DPA**) could encapsulate ferroceniums by complexation of the electron-donating skeleton of the DPA imines. Upon addition of ferroceniums to a series of dendritic polyphenylazomethines (**DPAG*X***, where *X* is the generation number, $X = 1-4$), the UV−vis spectra showed changes in a manner similar to that observed for the complexation of metal ions with **DPAG*X***. Stepwise shifts in the isosbestic point were consistently observed with the number of imine groups in the first and second layers of the generation-4 dendrimer (**DPAG4**). **DPAG2** and **DPAG3** were also found to trap 6 equiv of ferroceniums. To investigate the complexation, UV−vis spectroscopy, ^{57}Fe Mössbauer spectroscopy, electrospray ionization-mass spectroscopy (ESI-MS), cyclic voltammetry (CV), and fluorescence spectroscopy were performed. We confirmed that neutral ferrocenes cannot complex with the imine group while ferroceniums can. Utilizing the redox property of ferrocenes, we were able to electrochemically control the encapsulation and release of ferrocenes into the **DPA** in a manner similar to redox-responsive proteins such as ferritin. In addition to ferrocenes, oligoferrocenes could also be trapped in the DPA. The biferrocene cation(1+) was particularly suitable for electrochemical switching due to its stable mixed valence condition. The terferrocene dication(2+) encapsulated into **DPAG4** could be fabricated into a thin film, which exhibited the near-infrared absorption of an intervalence charge-transfer (IV-CT) band, pointing the way toward the use of such systems in material science.

Introduction

Dendrimers[1] are highly branched macromolecules often spherical in geometry that contain a nanospace, making them highly useful as nanocapsules or nanoreactors. They have a single molecular weight and unique dendritic structure, in which the density of each layer increases radially outward. The nanospace has been used to encapsulate drugs,[2] nanoparticles,[3] and electronic materials[4] among other applications. In particular, dendrimers incorporating metal ions[5] have received much attention as a type of novel organometallic catalyst. For instance, we reported that metal ions are complexed to the imine groups of dendritic polyphenylazomethines (**DPA**, Chart 1a) in a stepwise radial fashion based on the basicity gradient of imine groups.[6] In addition to their application as nanocapsules, dendrimers show interesting potential as metal−organic hybrid materials.

Chart 1. (a) Fourth Generation of Dendritic Polyphenylazomethine (**DPAG4**) and (b) Ferrocenium Hexafluorophosphate ($FcPF_6$)

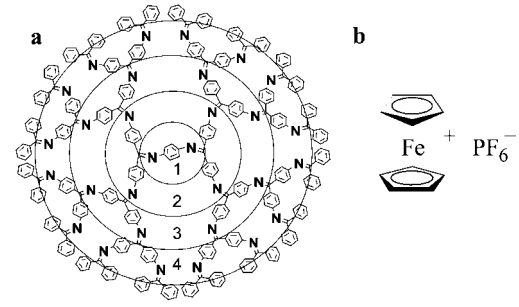

Ferrocene is a famous organometallic used for a variety of applications due to its useful redox property, stability, and synthetic convenience. This redox property has been utilized for sensors, surfactants, electronic materials, and even molecular machines.[7] In addition, the accumulation of the redox center has been investigated in relation to multielectron transfer,

[†] Keio University.
[‡] The University of Tokyo.
[§] Current Address: Chemical Resources Laboratory, Tokyo Institute of Technology, Yokohama 226-8503, Japan.

(1) (a) Newkome, G. R.; Yao, Z. Q.; Baker, G. R.; Gupta, V. K. *J. Org. Chem.* **1985**, *50*, 2003–2004. (b) Tomalia, D. A.; Baker, H.; Dewald, J.; Hall, H.; Kallos, G.; Martin, S.; Roeck, J.; Ryder, J.; Smith, P. *Polym. J.* **1985**, *17*, 117–132. (c) Grayson, S. M.; Fréchet, J. M. J. *Chem. Rev.* **2001**, *101*, 3819–3868. (d) Bosman, A. W.; Janssen, H. M.; Meijer, E. W. *Chem. Rev.* **1999**, *99*, 1665–1668. (f) Fischer, M.; Vögtle, F. *Angew. Chem., Int. Ed.* **1999**, *38*, 884–905.
(2) (a) Ambade, A. V.; Savariar, E. N.; Thayumanavan, S. *Mol. Pharmacol.* **2005**, *2*, 264–272. (b) Copper, A. I.; Londono, J. D.; Wignall, G.; McClain, J. B.; Samulski, E. T.; Lin, J. S.; Dobrynin, A.; Rubinstein, M.; Burke, A. L. C.; Fréchet, J. M. J. *Nature* **1997**, *389*, 368–371. (c) Morgan, M. T.; Carnahan, M. A.; Immoos, C. E.; Ribeiro, A. A.; Finkelstein, S.; Lee, S. J.; Grinstaff, M. W. *J. Am. Chem. Soc.* **2003**, *125*, 15485–15489.
(3) (a) Crooks, R. M.; Zhao, M.; Sun, L.; Chechik, V.; Yeung, L. K. *Acc. Chem. Res.* **2001**, *34*, 181–190. (b) Satoh, N.; Nakashima, T.; Kamikura, K.; Yamamoto, K. *Nat. Nanotech.* **2008**, *3*, 106–111. (c) Yamamoto, K.; Imaoka, T.; Chun, W. J.; Enoki, O.; Katoh, H.; Takenaga, M.; Sonoi, A. *Nat. Chem.* **2009**, *1*, 397–402.

magnetic, and nonlinear optical devices.[8] While ferrocene is easily oxidized into ferrocenium, which acts as a 1-electron acceptor, its noncovalent sensitivity for various anions based on the hydrogen-bonding, electrostatic attraction, and topological effects has been investigated in previous studies of the ferrocenyl dendrimers.[9]

The redox property of ferrocenes is also related to such redox phenomena in organisms. One example is ferritin,[10] iron storage proteins found in the liver. In this system, the mechanism of encapsulation and release of iron is mediated by the redox properties of the iron within the protein shell. We previously reported the ferritin-like redox switching irons complexed on **DPA**.[11] Similarly, other researchers have attempted to create redox-active bioorganometallics or metalloproteins.[12] In comparison to the use of iron ions, ferrocene offers a convenient alternative for creating novel redox-responsive systems, because of the potential for the molecular design through common organic synthesis.

In terms of constructing metalloprotein-like macromolecules, a dendritic framework is ideal as it allows for a precise design. To date, the incorporation of a ferrocene into a dendrimer has mainly been attempted through covalent bonding to produce redox-active dendrimers, which produced the anion sensors and electrochromic batteries[9] using the enhanced redox ability, the insight of the dendritic effect to the electron transfer,[13] and applications such as catalysts.[5b] While these covalent approaches were performed, the noncovalent approach to incorporate ferrocenes into dendrimers, which produces a reversibility and simplicity for a molecular design, is a rare and interesting field. Various researches of reversible molecular recognition using famous molecular cages through noncovalent bonding have been reported, such as cyclodextrin, cucurbit[7]uril, and cyclophane, among others.[14] The application of noncovalent interaction and equilibrium becomes advantageous and interesting to utilize the fine reversible redox property of the ferrocene. In fact, the assembly of ferrocenes into a supramolecular dendrimer for anion sensors has been studied using hydrogen bonding without the multistep synthetic procedure by Astruc's group.[15] It is possible that the noncovalent approach of ferrocene assembly using dendrimers creates novel electrofunctional materials. Moreover, the electrochemically controlled storage of ferrocenes and its derivatives using the dendrimer interior and redox-active ferrocene is scientifically interesting and unprecedented to the best of our knowledge.

We demonstrated the novel and precise assembly of ferrocenes into **DPA**s utilizing the unique interaction between the nucleophilic π-conjugated Schiff bases, which is advantageous to holding cationic molecules[16] and oxidized ferroceniums (Fc^+, Chart 1b). We found that our higher generation of DPAs could encapsulate ferroceniums into the electron-donating layer of the dendrimer. Using the useful redox property of ferrocene, we succeeded in fine control of the electrochemical encapsulation and release of ferrocene and its derivatives, analogous to redox-responsive proteins, i.e., ferrtins. This reversible encapsulation/release switching using a dendrimer is a unique characteristic of this ferrocene assembly using its noncovalent approach and equilibrium condition. In addition to ferrocene, we were also able to encapsulate oligoferrocenes within **DPA**s. We were able to significantly obtain thin films of the amorphous **DPA** including the oligoferrocenes, which absorbed in the near-infrared. Biferrocenes, in particular, were found to be suitable for the fine reversible switching. The overall assemblies of the **DPA** complexes were investigated on the basis of the UV−vis absorption spectroscopy, ^{57}Fe Mössbauer spectroscopy, ESI-MS, CV, and fluorescence spectroscopy.

Results and Discussion

Assembly of Ferroceniums. We found that the ferrocenium in our system complexed with the nucleophilic **DPA** imines. The UV−vis spectra revealed that the ferrocenium complexed with **DPA**. When the UV−vis titration of ferrocenium hexafluorophosphate ($FcPF_6$) into a **DPA** was carried out, a distinct change was observed in the UV−vis spectra; that is, the absorption around 445 nm increased while the absorption around 300 nm, attributed to the imines, decreased.

(4) (a) Percec, V.; Glodde, M.; Bera, T. K.; Miura, Y.; Shiyanovskaya, I.; Singer, K. D.; Balagurusamy, S. K.; Heiney, P. A.; Schnell, I.; Rapp, A.; Spiess, H. W.; Hudson, D.; Duan, H. *Nature* **2002**, *419*, 384–388. (b) Kawa, M.; Fréchet, J. M. J. *Chem. Mater.* **1998**, *10*, 286–296.

(5) (a) Newkome, G. R.; He, E.; Moorefield, C. N. *Chem. Rev.* **1999**, *99*, 1689–1746. (b) Astruc, D.; Chardac, F. *Chem. Rev.* **2001**, *101*, 2991–3023. (c) Knapen, J. W. J.; van der Made, A. W.; de Wilde, J. C.; van Leeuwen, P. W. N. M.; Wijkens, P.; Grove, D. M.; van Koten, G. *Nature* **1994**, *372*, 659–663. (d) Zhao, M.; Sun, L.; Crooks, R. M. *J. Am. Chem. Soc.* **1998**, *120*, 4877–4878.

(6) (a) Yamamoto, K.; Higuchi, M.; Shiki, S.; Tsuruta, M.; Chiba, H. *Nature* **2002**, *415*, 509–511. (b) Higuchi, M.; Tsuruta, M.; Chiba, H.; Shiki, S.; Yamamoto, K. *J. Am. Chem. Soc.* **2003**, *125*, 9988–9997.

(7) (a) Beer, P. D. *Acc. Chem. Res.* **1998**, *31*, 71–80. (b) Bayly, S. R.; Beer, P. D.; Chen, G. Z. *Ferrocenes* **2008**, 281–318. (c) Kinbara, K.; Aida, K. *Chem. Rev.* **2005**, *105*, 1377–1400. (d) Donohue, J. J.; Buttry, D. A. *Langmuir* **1989**, *5*, 671–678. (e) Widring, C. A.; Miller, C. J.; Majda, M. *J. Am. Chem. Soc.* **1988**, *110*, 2009–2011. (f) Martin, N.; Sanchez, L.; Illescas, B.; Prez, I. *Chem. Rev.* **1998**, *98*, 2527–2548.

(8) (a) Murata, M.; Yamada, M.; Fujita, T.; Kojima, K.; Kurihara, M.; Kubo, K.; Kobayashi, K.; Nishihara, H. *J. Am. Chem. Soc.* **2001**, *123*, 12903–12904. (b) Nakagawa, H.; Ogawa, K.; Satake, A.; Kobuke, Y. *Chem. Commun.* **2006**, *15*, 1560–1562. (c) Nagayoshi, K.; Kabir, M. K.; Tobita, H.; Honda, K.; Kawahara, M.; Katada, M.; Adachi, K.; Nishikawa, H.; Ikemoto, I.; Kumagai, H.; Hosokoshi, Y.; Inoue, K.; Kitagawa, S.; Kawata, K. *J. Am. Chem. Soc.* **2003**, *125*, 221–232. (d) Li, G.; Song, Y.; Hou, H.; Li, L.; Fan, Y.; Zhu, Yu.; Meng, X.; Mi, L. *Inorg. Chem.* **2003**, *42*, 913–920.

(9) (a) Valério, C.; Fillaut, J.; Ruiz, J.; Guittard, J.; Blais, J.; Astruc, D. *J. Am. Chem. Soc.* **1997**, *119*, 2588–2589. (b) Ornelas, C.; Aranzaes, J. R.; Cloutet, E.; Alves, S.; Astruc, D. *Angew.Chem., Int. Ed.* **2007**, *46*, 872–877. (c) Ormelas, C.; Ruiz, J.; Belin, C.; Astruc, D. *J. Am. Chem. Soc.* **2009**, *131*, 590–601. (d) Ornelas, C.; Ruiz, J.; Astruc, D. *Organometallics* **2009**, *28*, 4431–4437.

(10) (a) Kaim, W.; Schwederski, B. *Bioinorganic Chemistry: Inorganic Elements in the Chemistry of Life: An Introduction and Guide*; Wiley: England, 1994. (b) Dougas, T.; Dickson, D. P. E.; Betteridge, S.; Charnock, J.; Garner, C. D.; Mann, S. *Science* **1995**, *269*, 54–57. (d) Liu, X.; Theil, E. C. *Acc. Chem. Res.* **2005**, *38*, 167–175. Crow, A.; Lawson, T. L.; Lewin, A.; Moore, G. R.; Le Brun, N. E. *J. Am. Chem. Soc.* **2009**, *131*, 6808–6813.

(11) Nakajima, R.; Tsuruta, M.; Higuchi, M.; Yamamoto, K. *J. Am. Chem. Soc.* **2004**, *126*, 1630–1631.

(12) (a) Staveren, D. R. V.; Metzler-Nolte, N. *Chem. Rev.* **2004**, *104*, 5931–5986. (b) Lu, Y.; Berry, S. M.; Pfister, T. D. *Chem. Rev.* **2001**, *101*, 3047–3080. (c) Hwang, H. J.; Carey, J. R.; Brower, E. T.; Gengenbach, A. J.; Abramitge, J. A.; Lu, Y. *J. Am. Chem. Soc.* **2005**, *127*, 15356–15357.

(13) (a) Cardona, C. M.; Mendoza, S.; Kaifer, A. E. *Chem. Soc. Rev.* **2000**, *29*, 37–42. (b) Stone, D. L.; Smith, D. K.; McGrail, P. T. *J. Am. Chem. Soc.* **2002**, *124*, 856–864. (c) Appoh, F. E.; Thomas, D. S.; Kraatz, H. B. *Macromolecules* **2005**, *38*, 7562–7570. (d) Cardona, C. M.; Kaifer, A. E. *J. Am. Chem. Soc.* **1998**, *120*, 4023–4024.

(14) (a) Kaifer, A. E. *Acc. Chem. Res.* **1999**, *32*, 62–71. (b) Matue, T.; Evans, D. H.; Osa, T.; Kobayashi, N. *J. Am. Chem. Soc.* **1985**, *107*, 3411–3417. (c) Ong, W.; Kaifer, A. E. *Organometallics* **2003**, *22*, 4181–4183. (d) Seward, E. M.; Hopkins, R. B.; Sauerer, W.; Tam, S. W.; Diederich, F. *J. Am. Chem. Soc.* **1990**, *112*, 1783–1790.

(15) (a) Daniel, M. C.; Ruiz, J.; Astruc, D. *J. Am. Chem. Soc.* **2003**, *125*, 1150–1151. (b) Daniel, M. C.; Ba, F.; Ruiz, J.; Astruc, D. *Inorg. Chem.* **2004**, *43*, 8649–8657.

(16) Jiang, J.; MacLachlan, M. J. *Chem.Commun.* **2009**, *38*, 5695–5697.

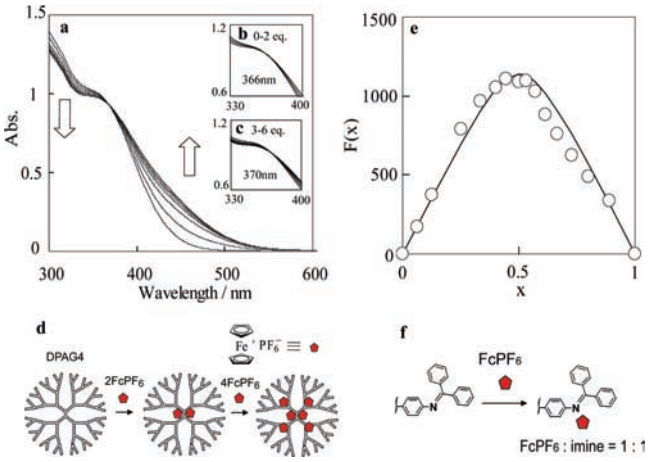

Figure 1. UV−vis spectra of **DPAG4** complexed with (a) 0−6, (b) 0−2, and (c) 3−6 equiv of $FcPF_6$ (solvent, $CHCl_3/CH_3CN$ = 1/1, [**DPAG4**] = 5×10^{-6} M). (d) Schematic representation of the encapsulation of DPAG4 with $FcPF_6$. (e) Job plot of $FcPF_6$ and **DPAG1** based on the changes in the UV−vis spectra. The equilibrium constant of complexation, *K*, obtained by curve-fitting using a theoretical simulation of the experimental data was 1.3×10^5 M^{-1}. (f) Schematic representation of the complexation of a **DPAG1** imine and $FcPF_6$.

A UV−vis titration was performed by the addition of $FcPF_6$ to **DPAG4** in a $CHCl_3/CH_3CN$ = 1:1 solution (Figure 1a). During the addition of 6 equiv of $FcPF_6$, isosbestic points were observed at 366 nm from 0−2 equiv of $FcPF_6$ and at 370 nm from 3−6 equiv of $FcPF_6$, indicating complexation within the first and second layer imines, respectively, due to the higher electron density of the inner imines.[6] After the addition of 6 equiv of $FcPF_6$, there were few additional spectral changes, which is in contrast to that for metals. A similar assembly process occurred in the cases of **DPAG2** and **DPAG3** (Figure S1, Supporting Information). For **DPAG2**, two isosbestic points, at 343 and 351 nm, were apparent after the addition 0−2 and 3−6 equiv of $FcPF_6$, respectively. In the case of **DPAG3**, two isosbestic points, centered at 375 nm and 368 nm, were apparent after the addition of 0−2 and 3−6 equiv of $FcPF_6$, respectively. A Job plot[17] of **DPAG1** and $FcPF_6$ showed a maximum at the 0.5 mol fraction of $FcPF_6$, which indicates that the imine forms a 1:1 complex with $FcPF_6$ (Figure 1e). The equilibrium constant of the complexation, *K*, was determined to be 1.3×10^5 M^{-1} by curve fitting using a theoretical simulation of the experimental data by the Job plot and titration curve (Figure S2, Supporting Information). In contrast, the UV−vis spectra of **DPA** with neutral ferrocenes did not change, which suggested no interaction. In addition in the change of the **DPA** absorption, the ferrocenium absorption at 620 nm decreased in proportion to the complexation with an imine (Figure S3, Supporting Information).

For the metal assembly, an imine coordinates with a metal salt based on the Lewis acid and base interaction. However, ferrocenium is a 17-electron system complex, which cannot make a complete coordinate bond with a 2-electron donor imine. In this study, the charge-transfer (CT) interaction[18] is the driving force of the ferrocenium assembly. In fact, similar CT complexes including ferrocene compounds or other metallocene compounds have been reported.[19] High equilibrium constants similar to the ferrocenium **DPA** complex ($\sim 10^5$ M^{-1}) have been reported in CT ion pairs.[18a,19c,20] Moreover, π-conjugated molecules containing nitrogen can also make CT complexes.[21] In addition to these previous studies, the change in the UV−vis spectra of DPA (Figure 1) and the ferroceniums[22] (Figure S3, Supporting Information) and ^{57}Fe Mössbauer spectra described in the following section indicated their CT interaction. The increase in the UV−vis spectra of the DPA complexed with ferroceniums was observed at almost the same wavelength (445 nm) as that of the metal-complexed **DPAG4**. This similar change indicated that an unshared electron pair of the imine nitrogen interacts with a ferrocenium, which supports the stepwise radial complexation based on the higher electron density of the inner imines.[6]

In terms of the ferrocenium counteranion, weakly coordinating anions[23] were found to be suitable for the complexation of ferrocenium with **DPA** to avoid any competition due to an electrostatic attraction.[9d] The equilibrium constants of $FcPF_6$, $FcBF_4$, and $FcBPh_4$ were determined by curve fitting using a titration curve with **DPAG1** (Figure S4, Supporting Information): $K_{FcPF6} = 1.3 \times 10^5$ $M^{-1} > K_{FcBF4} = 1.5 \times 10^4$ $M^{-1} > K_{FcBPh4} = 7.0 \times 10^2$ M^{-1}. In addition, the ^{19}F-NMR chemical shifts of PF_6^- and BF_4^- showed the shifts before and after complexation of the ferrocenium with **DPA** (Figure S5, Supporting Information). PF_6^- and BF_4^- showed the upfield shift of 0.7 ppm and the downfield shift of 2.0 ppm, respectively, the chemical shifts of which after complexation became almost the same ppm as tetrabutylammonium (TBA)PF_6 and $TBABF_4$. These results suggest that the moderate dissociation of a counteranion from a ferrocenium[24,25] is important for the complexation of ferroceniums with a **DPA**.

(17) $F(x) = \text{Abs}/(C_{G0} + C_{FcPF6}) - (\varepsilon_{G0} - \varepsilon_{FcPF6})x - \varepsilon_{FcPF6}$, $x = C_{G0}/(C_{G0} + C_{FcPF6})$; *x* is the molar fraction of **DPAG1**. Chloroform/acetonitrile (1/1) solution of **DPAG1** (2.0×10^{-4} M based on imine) and $FcPF_6$ with the same concentration were mixed in various proportions. The plot shows a maximum at a 0.5 mol fraction of **DPAG1**, which means that the imine forms a 1:1 complex with $FcPF_6$.

(18) (a) Hubig, S. M.; Kochi, J. K. In *Electron Transfer in Chemisry*; Balzani, V., Astruc, D., Eds.; Wiley-VCH: Germany, 2001; Vol. II, p 618−671. (b) Rosokha, S. V.; Kochi, J. K. *Acc. Chem. Res.* **2008**, *41*, 641–653.
(19) (a) Lehmann, R. E.; Kochi, J. K. *J. Am. Chem. Soc.* **1991**, *113*, 501–512. (b) Veya, P. L.; Kochi, J. K. *J. Organomet. Chem.* **1995**, *488*, C4–C8. (c) Bockman, T. M.; Kochi, J. K. *J. Am. Chem. Soc.* **1989**, *111*, 4669–4683. (d) Rosenblum, M.; Fish, R. W.; Bennett, C. *J. Am. Chem. Soc.* **1964**, *86*, 5166–5170.
(20) Schramm, C.; Zink, J. I. *J. Am. Chem. Soc.* **1979**, *101*, 4554–4558.
(21) (a) Zhu, D.; Kochi, J. K. *Organometallics* **1999**, *18*, 161–172. (b) Blackstock, S. C.; Kochi, J. K. *J. Am. Chem. Soc.* **1987**, *109*, 2484–2496.
(22) Similar disappearance of ferrocenium cation absorption (Figure S4, Supporting Information) has been observed, for instance, in the case of the CT complex of Fc/TCNE system (ref 19d). Unfortunately, a new CT absorption could not be identified clearly because the new CT absorption would exist near the $\pi-\pi^*$ large absorption of imines (445nm, $\varepsilon = 10^4$ M^{-1} cm^{-1}), much smaller and broader than **DPA** absorption ($\sim$500 nm, $\varepsilon = \sim 10^2$ M^{-1} cm^{-1}), expected from similar CT complexes (refs 19a and 19c).
(23) Strauss, S. H. *Chem. Rev.* **1993**, *93*, 927–942.
(24) We anticipate that the counteranions are in a relatively free state inside or near a **DPA** molecule within the electrostatic limitation shown by ESI-MS (Figure S8b, Supporting Information) due to the weakly coordinating anion, the wide space inside **DPA** (Table S1, Supporting Information, refs 25a and 25b), and less back folding of the **DPA** rigid structure (refs 25c and 25d).
(25) (a) Imaoka, T.; Tanaka, R.; Yamamoto, K. *Chem.−Eur. J.* **2006**, *12*, 7328–7336. (b) Fujii, A.; Ochi, Y.; Nakajima, R.; Yamamoto, K. *Chem. Lett.* **2009**, *38*, 418–419. (c) Messina, R.; Maiti, P. K. *Macromolecules* **2008**, *41*, 5002–5006. (d) Higuchi, M.; Shiki, S.; Ariga, K.; Yamamoto, K. *J. Am. Chem. Soc.* **2001**, *123*, 4414–4420.

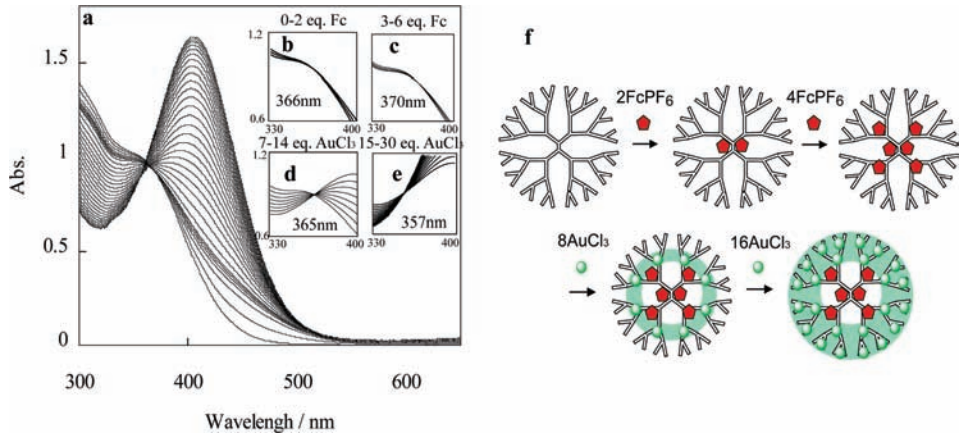

Figure 2. UV−vis spectra of **DPAG4** complexed with (a) 6 equiv of $FcPF_6$ and 24 equiv of $AuCl_3$, (b) 0−2 equiv of $FcPF_6$ and 2equiv of $FcPF_6$, (c) 3−6 equiv of $FcPF_6$ and 4 equiv of $FcPF_6$, (d) 7−14 equiv of $FcPF_6$ and 8 equiv of $AuCl_3$, and (e) 15−30 equiv of $FcPF_6$ and 16 equiv of $AuCl_3$ (solvent, $CHCl_3/CH_3CN$ = 1/1. [**DPAG4**] = 5×10^{-6} M). (f) Schematic representation of the stepwise radial complexation of **DPAG4** with $FcPF_6$ and $AuCl_3$.

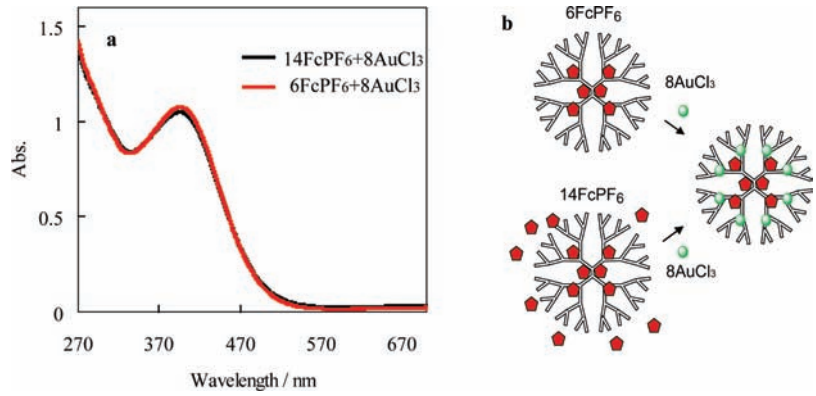

Figure 3. (a) UV−vis spectra of **DPAG4** complexed with 14 equiv of $FcPF_6$ and 8 equiv of $AuCl_3$, 6 equiv of $FcPF_6$ and 8 equiv of $AuCl_3$ (solvent, $CHCl_3/CH_3CN$ = 1/1. [**DPAG4**] = 5×10^{-6} M). (b) Schematic representation of the heterocomplexation: $14FcPF_6 + 8AuCl_3$ and $6FcPF_6 + 8AuCl_3$.

We reported that various kinds of metal salts can be located on a **DPAG4** through a stepwise radial complexation.[26] Using this unique heteroassembly, we further investigated the complexation of ferroceniums on the first and second layers of **DPAG4**. To confirm the assembly of ferroceniums on the first and second layers, we demonstrated that **DPAG4** encapsulating 6 equiv of ferroceniums was complexed with a quantity of $AuCl_3$, which forms a 1:1 complex with **DPA** imines,[27] consistent with the filling of the third and fourth layers of **DPAG4** (Figure 2). That is, after adding 6 equiv of ferroceniums to **DPAG4**, giving rise to two isosbestic points, 24 equiv of $AuCl_3$ could be added with two isosbestic points, observed at 8 and 16 equiv, respectively, corresponding to the filling of the third and fourth layers. As a control experiment, after adding 14 equiv of ferroceniums to **DPAG4**, 24 equiv of $AuCl_3$ was added, and again, two isosbestic points were observed at 8 and 16 equiv. In addition, the UV−vis spectra of the $14FcPF_6$ system with $8AuCl_3$ corresponded to that of the $6FcPF_6$ system with $8AuCl_3$ (Figure 3). These results confirm that 6 equiv of ferrocenium is complexed with the first and second layers of **DPAG4**. The same conclusion was obtained using $SnCl_2$ instead of $AuCl_3$.

The previously reported CT complexes of the ferrocene compounds show that the average distance between the donor and acceptor is 3−4 Å.[19] From the equilibrium condition of the ferrocenium and imine with a relatively high interaction ($K = 10^5\ M^{-1}$), a complexed ferrocenium is probably located within 3−4 Å from an inner imine site. The radius of **DPAG4** is 15 Å, and the average distances from the first and second layers of the imine site to the outer shell are 14 and 8 Å, respectively.[10] Taking these molecular distances into consideration, the ferroceniums complexed with the inner imines of **DPAG4** are sufficiently encapsulated into the dendrimer molecules.

Next, we performed the titrations using the half-substituted **DPA**, represented as **Half-DPAG*X*** (X = 3, 4), which has less dendritic effects on the difference between the inner and the outer microenvironments[28] than those for **DPAG4** (Chart S1, Supporting Information). Although the change in absorption was lower than that observed for metal salts, four changes in the position of the isosbestic points could be observed for **Half-DPAG4** (Figure S6, Supporting Information). This result suggests that the ferroceniums are able to interact with the outer layers of the **Half-DPAG4** and **Half-DPAG3** to some degree. Considering these results of **Half-DPA**, the limited Fc^+ assembly on the third and fourth layers of **DPAG4** is attributed to the dendritic shielding effects[28] or the different molecular

(26) Takanashi, K.; Fujii, A.; Nakajima, R.; Chiba, H.; Higuchi, M.; Einaga, Y.; Yamamoto, K. *Bull. Chem. Soc. Jpn.* **2007**, *80*, 1563–1572.
(27) Takanashi, K.; Ochi, Y.; Yamamoto, K. Manuscript in preparation.
(28) (a) Hecht, S.; Fréchet, J. M. J. *Angew. Chem., Int. Ed.* **2001**, *40*, 74–91. (b) Harth, E. M.; Hecht, S.; Helms, B.; Malmstrom, E. E.; Fréchet, J. M. J. *J. Am. Chem. Soc.* **2002**, *124*, 3926–3938.

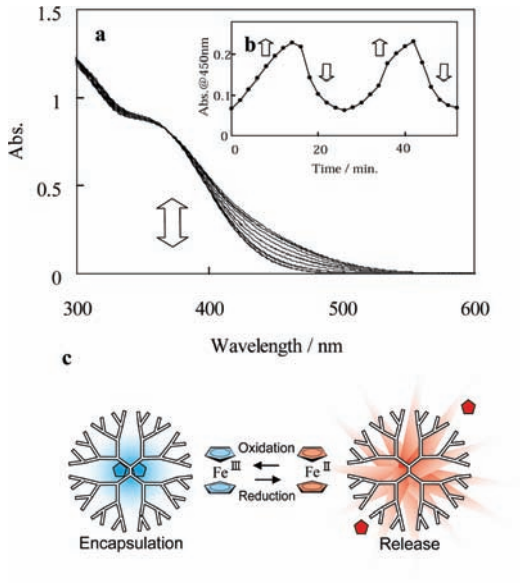

Figure 4. (a) Electro-UV−vis spectral changes of **DPAG4** complexed with 2 equiv of ferroceniums, **$(FcPF_6)_2$@DPAG4**. [**DPAG4**] = 5×10^{-5} M, [Fc] = 1×10^{-4} M, [$TBAPF_6$] = 0.2 M, from +0.2 to −0.25 V vs Ag/Ag^+. (b) Absorption changes at 450 nm. The absorption change during release is fitted to be first-order kinetics ($k_1 = 8.0 \times 10^{-4}$ s^{-1}). The complexation is fitted to be second-order kinetics ($k_2 = 32$ s^{-1} M^{-1}). (c) Schematic representation of the electrochemical encapsulation/release of the ferrocenes.

motion between the inner and outer backbones.[29] We expect that this different Fc^+ behavior from that of the metal assembly is also due to the environmental sensitivity[19a] or the greater distance between the Fc^+−imine than the metal−imine coordination, which are typical characteristics of a charge-transfer complex.

Whereas a ferrocenium could be coordinated to the **DPA** imines, the neutral ferrocene was not. By taking advantage of this property, we could control the reversible electrochemical encapsulation and release of the ferrocenes. Specifically, the UV−vis absorption at around 445 nm of the **DPA** imines was increased at a potential of 0.2 V vs Ag/Ag^+ for 15 min, whereas the absorption decreased at −0.25 V for 10 min, indicating the encapsulation and release of the ferrocenes (Figure 4). A relatively long equilibration was required to complete the assembly and release because of the diffusion-limited access to the electrode. As a control experiment, a **DPAG4** solution was measured without ferrocenes, and no changes were observed in the UV−vis spectra under the same conditions. Although switching behavior was observed, the switching gradually became irreversible as a result of the exposure to high voltage over a long time or after many cycles of switching, presumably due to decomposition. Thus, switching of the encapsulation/release of ferrocene was limited, occurring only for a relatively short time and after only a few cycles, two at most. Considering the reaction rate of the switching, the release by the Fc^+ reduction ($k_1 = 8.0 \times 10^{-4}$ s^{-1}) was faster than that of the encapsulation by the Fc oxidation ($k_2 = 32$ s^{-1} M^{-1}). A similar behavior was also observed in the case of biferrocene switching (60 min for encapsulation; $k_2 = 10$ s^{-1} M^{-1}; 30 min for release; $k_1 = 3.0 \times 10^{-4}$ s^{-1}) described in the following section. While the responsiveness of the complexation by the electrochemical oxidation seems to be less sensitive than that of the release for the previous sensors of ion-pairing ferrocenyl dendrimers,[9] probably due to the electrostatic competition by anions and the dendritic shielding effect, the release of the ferrocenes by the electrochemical reduction rapidly occurs.

In order to clarify the oxidation state and charge-transfer (CT) interaction of the ferroceniums encapsulated in **DPA**, we performed ^{57}Fe Mössbauer spectroscopy. To obtain the **$(^{57}FcPF_6)_2$@ DPAG4** species, we formed a complex of $^{57}FcPF_6$ and **DPAG4**, allowed it to reach an equilibrium, and then precipitated it into hexane. In the Mössbauer spectrum, **$(^{57}FcPF_6)_2$@DPAG4** showed a doublet spectrum, which indicated different isomeric shift (IS) and quadrupole splitting (QS) from that of $FcPF_6$ (IS = 0.31 mm·s^{-1}) or Fc (IS = 0.32 mm·s^{-1}, QS = 2.39 mm·s^{-1}) in isolation (Figure 5). The IS and QS values of **$(^{57}FcPF_6)_2$@DPAG4** were IS = 0.24 mm·s^{-1} and QS = 0.79 mm·s^{-1} at RT with the features broadening at 150 and 9 K (Figure S7, Supporting Information). This broad peak was caused by spin relaxation of the $3d^5$ orbital and suggests the low-spin state ($S = 1/2$) of an Fe^{3+}.[30] Almost the same IS and QS values were observed in the case of **$(^{57}FcPF_6)_6$@DPAG4**, which confirmed that 6 equiv of $FcPF_6$ could be encapsulated within **DPAG4** (Figure S7, Supporting Information). In the case of **$(^{57}FcPF_6)_2$@DPAG1**, a mixed spectra of **$(^{57}FcPF_6)_6$@DPA** and $FcPF_6$ was observed due to its poor encapsulating ability as a result of reprecipitation.

This change in the ^{57}Fe Mössbauer spectra confirms the CT interaction between a ferrocenium and a **DPA** imine, which is suggested by the discussion of the UV−vis spectrum investigation. The change in QS by the complexation is attributed to the charge delocalization and orbital overlap[31a,19c] between a ferrocenium and a **DPA** imine. In fact, similar ^{57}Fe Mössbauer spectra of the ferroceniums have been reported for the CT complexes of the previous ferrocenium compounds.[31] Moreover, the approach of nucleophilic species to the ferrocenophaniums has been also reported having similar ^{57}Fe Mössbauer spectra,[32] supported by the possibility of a nucleophilic interaction with the $2a_1$ molecular orbital of the ferrocene.[33,9d] These studies sufficiently support the CT interaction of the ferrocenium and **DPA**.

Characterization of the $FcPF_6$/**DPA** complex was also carried out by ESI-MS spectroscopy. It is difficult to detect the complexes of higher generation **DPA**s because of their low ionization activity. However, in the case of **DPAG1**, the complex of [**$(FcPF_6)$@DPAG1**+H^+] (calcd 768.2) was observed at 768.3 using a sample of the **DPAG1** solution in which 1 mol equiv of $FcPF_6$ was added (Figure S8, Supporting Information). The observed peak pattern (Figure S8b, Supporting Information) corresponded to the simulated peak pattern includ-

(29) (a) Higuchi, M.; Shiki, S.; Yamamoto, K. *Org. Lett.* **2000**, *2*, 3079–3082.
(30) Birchall, T.; Drummond, I. *Inorg. Chem.* **1971**, *10*, 399–401.
(31) (a) Kowalski, K.; Linseis, M.; Winter, R. F.; Zabel, M.; Záliš, S.; Kelm, H.; Krüger, H. J.; Sarkar, B.; Kaim, W. *Organometallics* **2009**, *28*, 4196–4209. (b) Mochida, T.; Takazawa, K.; Matsui, H.; Takahashi, M.; Takeda, M.; Sato, M.; Nishio, Y.; Kajita, K.; Mori, H. *Inorg. Chem.* **2005**, *44*, 8628–8641. (c) Kramer, J. A.; Hendrickson, D. N. *Inorg. Chem.* **1980**, *19*, 3330–3337. (d) Kaufmann, L.; Breunig, J. M.; Vitze, H.; Schödel, F.; Nowik, I.; Pichlmaier, M.; Bolte, M.; Lerner, H. W.; Winter, R. F.; Herber, R. H.; Wagner, M. *Dalton Trans.* **2009**, 2940–2950. (e) Liu, Y.; Tang, H.; Qin, J.; Inokuchi, M.; Kinoshita, M. *J. Inorg. Organomet. Polym. Mat.* **2007**, *17*, 111–119.
(32) (a) Watanabe, M.; Sato, K.; Motoyama, I.; Sano, H. *Chem. Lett.* **1983**, *11*, 1775–1778. (b) Watanabe, M.; Motoyama, I.; Sano, H. *J. Radioanal. Nucl. Chem.* **1985**, *6*, 585–592. (c) Ogino, H.; Tobita, H.; Habazaki, H.; Shimoi, M. *J. Chem. Soc., Chem. Commun.* **1989**, *13*, 828–829.
(33) Lauher, W.; Hoffmann, R. *J. Am. Chem. Soc.* **1976**, *98*, 1729–1742.

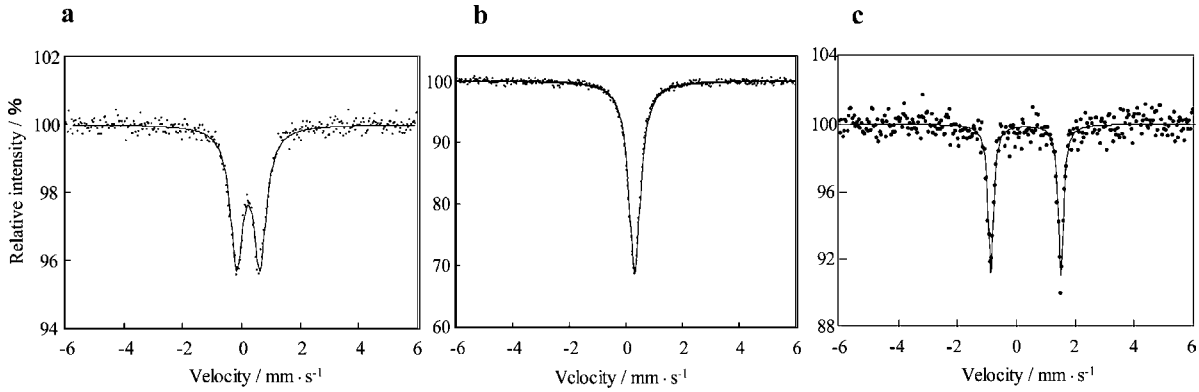

Figure 5. ^{57}Fe Mössbauer spectra of (a) **(FcPF$_6$)$_2$@DPAG4** (IS = 0.24 mm·s^{-1}, QS = 0.79 mm·s^{-1}), (b) FcPF$_6$ (IS = 0.32 mm·s^{-1}), and (c) ferrocene (IS = 0.32 mm·s^{-1}, QS = 2.39 mm·s^{-1}) at 294 K.

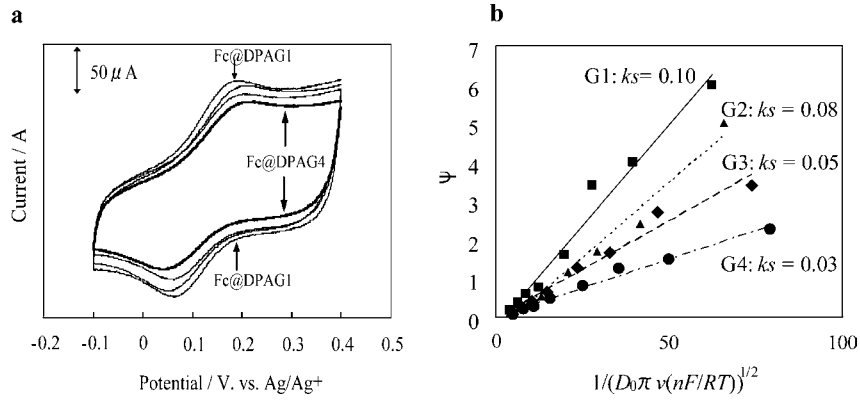

Figure 6. (a) Cyclic voltammograms of **DPAG*X*** ($X = 1-4$) complex with 1 equiv of FcBF$_4$ taken at the fast scan rate of 20 V/s. The curves are displayed in order from the inner curve to the outer one, **DPAG4**, **DPAG3**, **DPAG2**, and **DPAG1**, respectively. (b) Nichlson plots[36] for the electron-transfer rate constants *k*s of **(FcBF$_4$)@DPAG*X*** ($X = 1-4$).

ing Fe isotopes (Figure S8c, Supporting Information). Although other fragment peaks were observed (Figure S8a, Supporting Information), such as **DPAG**1, (**DPAG1**)$_2$, and (**DPAG1**)$_2$PF$_6$, this result suggested that a ferrocenium complexed with the DPA which was electrostatically stabilized by PF_6^-.

These results exclude the possibility of a side reaction of the ferroceniums, such as a simple oxidation or decomposition. Ferrocenium is known as a 1-electron oxidant in its reaction from ferrocenium to ferrocene. Significantly, no peaks corresponding to ferrocene were detected in the ^{57}Fe Mössbauer spectra or ESI-MS spectrum, which shows that the ferrocenium was not reduced through a 1-electron transfer. Decomposition of the ferrocenium by nucleophilic species was also excluded based on the absence of any ferrocene signals because the decomposition of ferrocenium is known to involve the formation of neutral ferrocene following reduction by $C_5H_5^-$ ions.[34] $Fc^+FeX_4^-$, a typical decomposed compound of ferrocenium, has asymmetric ^{57}Fe Mössbauer peaks, which clearly differs from our results.[35]

Ferrocene shows a reversible redox wave in the cyclic voltammogram. The encapsulation of ferrocenium into **DPA** was monitored by cyclic voltammetry, taking into account the difficulty in measuring the generation effect of dendrimers because of the rapid release by the reduction of ferroceniums into ferrocenes. To detect the influence of ferrocenes being released from DPA, a solution of **(FcBF$_4$)@DPAG*X*** ($X = 1-4$) was swept at a relatively fast scan rate (0.2−50 V·s^{-1}) by cyclic voltammetry (CV). FcBF$_4$, which complexed in a fashion similar to **DPA**, was selected in this experiment due to its reproducibility. In the CV, the higher generation dendrimers gave rise to a lower electric current and a wider peak separation (Figure 6a). These tendencies were attributed to the decrease in the diffusion constant and the electron-transfer rate constant caused by the increase in molecular size (**DPAG4**, 3.2 nm; **DPAG3**, 2.4 nm; **DPAG2**, 1.8 nm; **DPAG1**, 1.2 nm diameter). The electron-transfer rate constants *ks* were estimated using Nichlson's method[36] based on the peak separations (Figure 6b, **Fc@DPAG4**, 0.03 cm s^{-1}; **Fc@DPAG3**, 0.05 cm s^{-1}; **Fc@DPAG2**, 0.08 cm s^{-1}, **Fc@DPAG1**, 0.10 cm s^{-1}). The diffusion constants estimated by DigiSim[37] were as follows: **Fc@DPAG4**, 6.5×10^{-6} cm^2 s^{-1}; **Fc@DPAG3**, 7.5×10^{-6} cm^2 s^{-1}, **Fc@DPAG2**, 9.5×10^{-6} cm^2 s^{-1}; **Fc@DPAG1**, 10.5×10^{-6} cm^2 s^{-1}. Although the tendency was slightly weak due to the release of the ferrocenes and the noncovalent interaction, these results correspond to those observed for ferrocene-cored dendrimers[13b,d] in regard to the electron-transfer rate constant and the diffusion constant found in the encapsulation of a ferrocene.

(34) (a) Prins, R.; Korswagen, A. R.; Kortbeek, A. G. T. G. *J. Organomet. Chem.* **1972**, *39*, 335–344. (b) Holecek, J.; Handlir, K.; Klikorka, J.; Nguyen, D. B. *Collect. Czech. Chem. Commun.* **1979**, *44*, 1379–1387.
(35) Birchall, T.; Drummond, I. *Inorg. Chem.* **1971**, *10*, 399–401.
(36) Nicholson, R. *J. Anal. Chem.* **1965**, *37*, 1351–1355.
(37) Rudolph, M.; Reddy, D. P.; Felberg, S. W. *Anal. Chem.* **1994**, *66*, 589A.

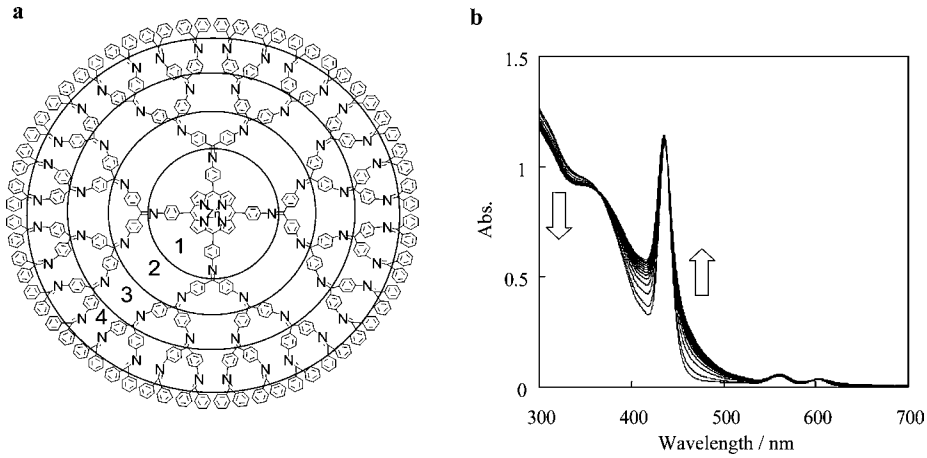

Figure 7. (a) Fourth generation of a phenylazomethine dendrimer with a zinc tetraphenylporphyrin core (**DPAG4-ZnP**). (b) UV−vis spectra of **DPAG4-ZnP** complexed with 0−12 equiv of $FcPF_6$ (solvent, $CHCl_3/CH_3CN$ = 1:1. [**DPAG4-ZnP**] = 2.5×10^{-6} M).

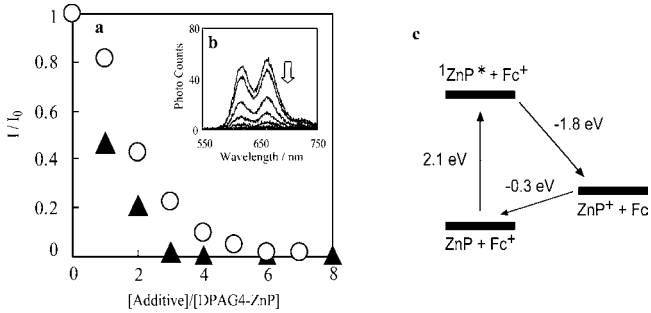

Figure 8. (a) Change in normalized fluorescence intensities of **DPAG4-ZnP** during the addition of $FcPF_6$ (○) or $FeCl_3$ (▲). (b) Fluorescence spectra of **DPAG4-ZnP** complexed with 0−8 equiv of $FcPF_6$. [**DPAG4-ZnP**] = 1×10^{-5} M. (c) Energy diagram for the oxidative quenching of a zinc porphyrin S1 state by $FcPF_6$.

The assembly of ferroceniums into a phenylazomethine dendrimer with a zinc tetraphenylporphyrin core (**DPAG4-ZnP**, Figure 7) was also performed. In the case of **DPAG4-ZnP**, although there was no obvious shift in the isosbestic point because of the small Soret-band shift, it was noted that the absorption at around 445 nm increased while the absorption at around 300 nm, attributed to the imine, decreased. No further changes were observed after the addition of 12 equiv of $FcPF_6$, which suggests that the **DPAG4-ZnP** also encapsulated ferroceniums up to the second layer, consistent with the **DPAG4** results (Figure 7).

The influence of the ferrocenium assembly on the fluorescence of **DPAG4-ZnP** was also investigated. The singlet excited state (S1) of **DPAG4-ZnP** is a weak oxidant (E = 0.4 V vs Ag/Ag^+) and a strong reductant (E = −1.7 V vs Ag/Ag^+). In addition, the ferrocene (E = 0.1 V vs Ag/Ag^+) is known to quench fluorescence.[38] Indeed, the fluorescence spectrum of **DPAG4-ZnP** upon excitation at the Soret band was completely quenched by the addition of the ferroceniums (Figure 8ab). This quenching behavior was similar to a previous report on the complexation of $FeCl_3$ (E = −0.1 V vs Ag/Ag^+) with **DPAG4-ZnP**.[39] These results indicate that electron transfer from the excited zinc porphyrin to the coordinating ferroceniums is promoted due to the higher reduction potential of the ferrocenes, in the same way as does $FeCl_3$ (Figure 8c). The difference in the quenching rate between the ferrocenium and $FeCl_3$ would depend on both the complexation constant and the reduction potential. As a control experiment, no quenching was observed when $FcPF_6$ was added to a solution of a zinc tetraphenylporphyrin (Figure S9, Supporting Information), which shows that the quenching effect was mediated through the **DPA** backbone. These results support the encapsulation of ferroceniums within the interior of the dendrimer.

Table 1. Complexation Constants and Redox Potentials of Ferroceniums and Oligoferroceniums

	$E_{1/2}$ (V vs Ag/Ag^+)	K (M^{-1})
Fc(+)	0.14	1.3×10^5
BiFc(+)	0.055, 0.40	1.5×10^3
TFc(2+)	−0.023, 0.18, 0.55	1.0×10^6

Expanding to Oligoferrocene Assembly. In addition to ferrocenes, we found that mixed valence oligoferrocenes could also be encapsulated into **DPA**. In particular, the biferrocene cation(1+) and terferrocene dication(2+), represented as BiFc(1+) and TFc(2+), respectively, were found to complex with **DPA**, whereas neutral oligoferrocenes did not interact with the imines.

For the assembly of BFc(1+), $BiFcPF_6$ was synthesized and added to a solution of **DPAG4**. The UV−vis spectra of the resulting solution showed that the absorption at around 445 nm increased while the absorption attributed to the imine decreased, which confirmed the interaction between $BiFcPF_6$ and the imines. BFc(1+) has a lower complexation constant (K_{BiFc} = ca. 1.5×10^3 M^{-1}, Figure S10, Supporting Information, Table 1) than the ferrocenium due to delocalization of a cation ($E_{1/2\ Fc+}$ = 0.14 V, $E_{1/2\ BiFc+}$ = 0.06 V vs Ag/Ag^+). The UV−vis titration was performed by addition of $BiFcPF_6$ using **DPAG4** (Figure 9a). During addition of 6 equiv of $BiFcPF_6$, isosbestic points were observed at 375 nm after 0−2 equiv of $BiFcPF_6$ and at 378 nm after 3−6 equiv of $BiFcPF_6$. Similar results were observed in the titration of **DPAG3** and **DPAG2** (Figure S11, Supporting Information). Although the complexation constant, K, of $BiFcPF_6$ is slightly lower than that of $FcPF_6$, it was also effectively encapsulated within the **DPA** in a manner similar to $FcPF_6$ due to the stronger basicity of the inner **DPA** imines when compared to the outer **DPA** imines.[6]

In terms of controlling the encapsulation and release, biferrocenes were found to be more suitable for reversible switching

(38) (a) Cao, W.; Ferrance, J. P.; Demas, J.; Landers, J. P. *J. Am. Chem. Soc.* **2006**, *128*, 7572–7578. (b) Geiber, B.; Alsfasser, R. *Inorg. Chim. Acta* **2003**, *344*, 102–108.

(39) Imaoka, T.; Tanaka, R.; Arimoto, S.; Sakai, M.; Fujii, M.; Yamamoto, K. *J. Am. Chem. Soc.* **2005**, *127*, 13896–13905.

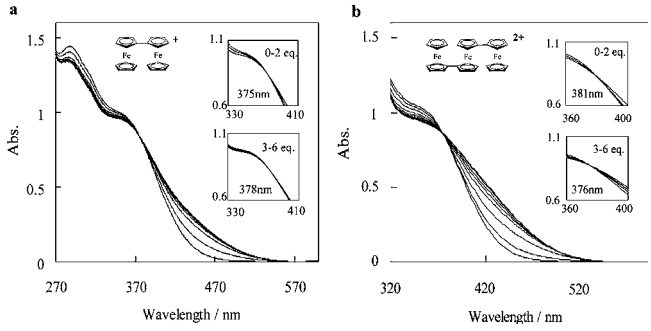

Figure 9. UV−vis spectra of **DPAG4** complexed with 0−6 equiv of (a) BiFc(1+) and (b) TFc(2+).

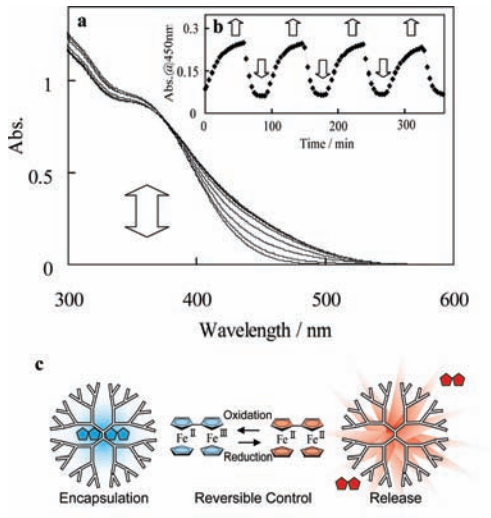

Figure 10. (a) Electro-UV−vis spectral changes in **(BiFc(1+))$_2$@DPAG4**. [**DPAG4**] = 5×10^{-5} M, [BiFc] = 1×10^{-4} M (solvent $CHCl_3$:CH_3CN = 1:1 with [$TBAPF_6$] = 0.2 M, the voltage switched from +0.2 to −0.25 V vs Ag/Ag^+). (b) Time-dependent change in **DPA** absorption at 450 nm with voltage switching. The absorption change during the release is fitted using first-order kinetics ($k_1 = 3.0 \times 10^{-4}$ s^{-1}). Complexation is fitted using second-order kinetics ($k_2 = 10$ s^{-1} M^{-1}). (c) Schematic representation of the electrochemical encapsulation/release of biferrocenes.

than the ferrocenes. As previously stated, the switching of ferrocenes was demonstrated only under a certain condition. Similarly, terferrocenes(2+) did not effectively release due to a higher redox potential than the other two ($E_{1/2\ TFc2+} = 0.18$ V). In contrast, the electro-UV−vis spectra showed that biferrocenes were stable and allowed many cycles (4 times at least) of the encapsulation and release (Figure 10) due to its charge delocalization and mild complexation. BiFc(1+) is indicated to be the most suitable species for a reversible encapsulation and release among the investigated ferrocene derivatives.

TFc(2+) was oxidized by 2 equiv of $FcCl_2PF_6$, before addition to the solution of **DPAG4**, because TFc(2+) was difficult to isolate as $TFc(PF_6)_2$. The UV−vis spectra of the **DPAG4** mixture showed that the absorption at around 445 nm increased while the absorption attributed to the imine decreased, which confirmed the interaction of the TFc(2+) and the imines (Figure 9b). The equilibrium constant of the complexation, *K*, was determined to be 1.0×10^6 M^{-1} by curve fitting of the **DPAG1** UV−vis spectra (Figure S10, Supporting Information), which had a relatively high complexation constant due to its high redox potential (Table 1, $E_{1/2\ TFc2+} = 0.14$ V, $E_{1/2\ TFc+} = -0.02$ V vs Ag/Ag^+). The UV−vis spectral results indicate that **DPAG4** is able to encapsulate relatively large TFc or BiFc molecules due to the inner wide space of the **DPA**,[25a,b] which was supported by the estimated free volume in a **DPAG4** molecule using the van der Waals volumes and hydrodynamic volume (Table S1, Supporting Information). However, TFc(+) had a weak complexation behavior because of its low redox potential, thus making it unsuitable for assembly.

In the encapsulation of TFc(2+), an IV-CT band in the near-infrared was observed. The IV-CT band gradually disappeared over a long time due to electron donation or charge localization by the **DPA** imine. As compared to BiFc(+), the IV-CT band of TFc(2+) was found to be relatively stable (Figure S12, Supporting Information). Interestingly, TFc(2+), which could not form a self-standing film, was able to form a thin film after encapsulation into **DPAG4** exhibiting an IV-CT band. In this process, a solution of TFc(2+) and **DPAG4** (1.5 mM, C_6H_5Cl/CH_3CN = 1:1 as solvent) was cast on a glass plate to form a thin film (Figure S13, Supporting Information), the thickness of which was ca. 1 μm in this experiment. We confirmed that the IV-CT band of the mixed valence terferrocenes in this film was stable for over 7 days. Consequently, the TFc(2+)-assembled **DPAG4** was shown to be suitable for application as near-infrared responsive materials, and further investigations are now in progress.

Conclusion

DPA is able to encapsulate ferroceniums into their inner layers. Specifically, 6 equiv of ferrocenium was trapped in the first and second layers of **DPA**. Electrochemical switching of the encapsulation/release of ferrocene was accomplished similarly to the redox-responsive protein. Not only ferrocenes but also oligoferrocenes, which form mixed valence states, are able to complex with the **DPA** imines and improve its functionality as an electrofunctional material. In terms of encapsulation/release switching, biferrocenes are proved to be the most suitable among the investigated ferrocenes. Moreover, a thin film of terferrocenes encapsulated in **DPA** exhibited an IV-CT band, indicating the potential for application of such complexes as infrared-responsive materials.

This study expands the range of species which can be encapsulated into **DPA** from metal ions to organometallics. Ferrocene is a redox-active metallocene and can be easily modified by various functional groups for the encapsulation/release of other functional molecules into **DPA**. Utilizing the electron density gradient of **DPA**, the storage of ferroceniums into **DPA** is unique from the standpoint of the electrochemical control of the reversible encapsulation/release system. Taking advantage of the noncovalent approach, we showed the convenient versatility of this system for other ferrocene derivatives, biferrocenes and terferrocenes, in this study. The application of this system for other metallocenes, ferrocene-attached derivatives, and various kinds of acceptors will be expected. Such methods will offer a route to the creation of novel intelligent materials, such as drug delivery systems, catalysis, or electrofunctional materials, as systems analogous to redox-responsive proteins.

Experimental Section

Methods. UV−vis spectra were recorded using a Shimadzu UV-3100PC spectrometer with a sealed quartz cell (optical path length 1 cm) at 293 K. Details of the UV−vis titration method are described in the following section General Method of UV−vis Titration.

Electro-UV−vis spectra monitoring of the encapsulation and release was carried out in chloroform/acetonitrile = 1:1 solvent mixture (**DPAG4** 5.0×10^{-5} M, 0.2 M $TBAPF_6$) after N_2 bubbling for 5 min. An UV−vis spectrometer (Shimazu UV-3100), a potentiostat (Hokuto Denko Co., Ltd., HA-501G), and a specially made thin layer cell (optical path length 1 mm) with a platinum-mesh electrode were used for the experiments. In the case of ferrocene, the oxidation was done at 0.2 V (vs Ag/Ag^+) for 15 min and reduction at −0.25 V (vs Ag/Ag^+) for 10 min. In the case of biferrocene, the oxidation was done at 0.2 V (vs Ag/Ag^+) for 60 min and reduction at −0.25 V (vs Ag/Ag^+) for 30 min.

The cyclic voltammetry experiments were carried out using an ALS 445 electrochemical analyzer. As the working electrode, a glassy carbon electrode ($\phi = 3$ mm) was used, which was polished with 0.05 mm alumina paste before analysis. The counter and the reference electrodes were Pt wire and Ag/Ag^+, respectively. All measurements were carried out with the same Ag/Ag^+ reference after N_2 bubbling for 5 min. The measurement solution was 2 mL of $CHCl_3$:CH_3CN = 1:1 including 0.1 M $TBABF_4$. The concentration of $FcBF_4$ in each solution was 0.5 mM, and equimolar quantities of **DPAG*X*** ($X = 1-4$) were added.

The ^{57}Fe Mössbauer spectra were measured using a Topologic systems model 222 constant-acceleration spectrometer. The data were recorded on a 1024-channel pulse height analyzer. The spectra were analyzed by fitting a Lorentzian line shape using MOSSWINN version 3 software. All samples were prepared using $^{57}FcPF_6$. The samples of **$(FcPF_6)_2$@ DPAG4** were prepared by reprecipitation from hexane.

The ESI-mass spectra were recorded by a JEOL JMS-T100CS using the **$(FcPF6)_2$@DPAG1** complex in chloroform/acetonitrile = 1:1 solvent mixture at 1 mM concentration.

The fluorescence spectra were measured by a Hamamatsu Photonics C9920−02 absolute PL quantum yield measurement system at room temperature. The concentration of the chloroform/acetonitrile solution was 10 μM, and the excitation wavelengths were 436 (**DPAG4-ZnP**) and 423 nm (**ZnTPP**) (Soret band of porphyrin). The titration method was similar to the UV−vis titration method.

The ^{19}F-NMR spectra were recorded using a JEOL ECX-400 FT-NMR spectrometer (400 MHz) in a CH_2Cl_2/CD_3CN = 4:1 solution for obtaining a sufficient solubility, and TFA was used as the external standard. The ^{1}H NMR spectra were recorded using a JEOL JMN400 FT-NMR spectrometer (400 MHz) in a $CDCl_3/CD_3CN$ = 1:1 + TMS (internal standard) solution. The concentration of **DPAG0** was 2 mM in the $BiFcPF_6$ experiment.

Chemicals. All **DPAs** were synthesized by a previously reported method.[40] The dehydrated chloroform was purchased from Wako Pure Chemical Industries, and the dehydrated acetonitrile and ferrocene were purchased from Kanto Kagaku Co. Ferrocenium hexafluorophosphate ($FcPF_6$) and ferrocenium tetrafluoroborate ($FcBF_4$) were purchased from Aldrich. Ferrocenium tetrafluoroborate ($FcBPh_4$) was synthesized by a previous method.[41] ^{57}Fe was purchased from TANGO OVERSEAS, and $^{57}Fe(Cp)_2$ was synthesized from $^{57}FeCl_2$ using a previous method.[42] Biferrocene and terferrocene were synthesized by a literature method.[43] Biferrocenium(1+) hexafluorophosphate and $FcCl_2PF_6$ were also synthesized by a literature method.[44,45] The terferrocene(2+) dication was prepared by addition of 2 equiv of $FcCl_2PF_6$ to an acetonitrile solution. All other chemicals were purchased from the Kanto Kagaku Co.

General Method of UV−vis Titration. Solutions of **DPAG4** (chloroform/acetonitrile = 1:1, $5:0 \times 10^{-6}$ M) and $FcPF_6$ (acetonitrile, 2.5×10^{-3} M) were prepared in volumetric flasks. To a 3.0 mL amount of the **DPAG4** solution in a quartz cell was immediately added 6 μL of a freshly prepared $FcPF_6$ solution (i.e., 1 equiv for **DPAG4**). The UV−vis spectra were measured until the absorbance change was converged. Measurements were repeated after each addition of 6 μL of $FcPF_6$ solution to achieve the UV−vis titration. After measurement of the UV−vis spectra, the absorption spectra of the additives ($FcPF_6$, $BiFcPF_6$, TFc(2+), $AuCl_3$) were subtracted to identify the changes in the DPA absorption and isosbestic points.[10,17] In the titration curves of **DPAG1**, the curve fitting with a theoretical simulation as a second-order reversible reaction was used.[26]

Acknowledgment. The authors extend their gratitude to JEOL, Ltd., for the ESI-mass spectroscopy measurements and to Mr. K. Oshida for his help with the ^{57}Fe Mössbauer spectroscopy measurements. We also thank Dr. N. Satoh, Mr. K. Albrecht, and Ms. R. Nakajima for their useful suggestions. This work was supported by Grants-in-Aid for Scientific Research (nos. 19205020, 21108009, 21750152), and Mitsubishi and Futaba Foundations.

Supporting Information Available: Additional UV−vis spectra, ^{57}Fe Mössbauer spectra, ESI-MS and NMR data, and additional data for the ferrocenium and oligoferrocene cation assembly. This material is available free of charge via the Internet at http://pubs.acs.org.

JA9064377

(40) Takanashi, K.; Chiba, H.; Higuchi, M.; Yamamoto, K. *Org. Lett.* **2004**, *6*, 1709–1712.

(41) Piglosiewicz, I. M.; Beckhaus, R.; Wittstock, G.; Saak, W.; Hasse, D. *Inorg. Chem.* **2007**, *46*, 7610–7620.

(42) Pray, A. R. *Inorg. Synth.* **1957**, 153–156.

(43) Hirao, T.; Kurashima, M.; Aramaki, K.; Nishihara, H. *J. Chem. Soc., Dalton Trans.* **1996**, 2929–2933.

(44) Dong, T. Y.; Kambara, T.; Hendrickson, D. N. *J. Am. Chem. Soc.* **1986**, *108*, 4423–4432.

(45) Horikoshi, T.; Kubo, K.; Nishihara, H. *J. Chem. Soc., Dalton Trans.* **1999**, 3355–3360.